

Supplemental Materials

Molecular Biology of the Cell

Costa et al.

Supplemental

csi2p modulates microtubule dynamics and organizes the bipolar spindle for chromosome segregation.

Judite Costa ^{1,2}, Chuanhai Fu ³, V. Mohini Khare ¹, Phong T. Tran ^{1,2}

¹ Department of Cell & Developmental Biology, University of Pennsylvania, Philadelphia PA 19104 USA

² Institut Curie, UMR 144 CNRS, Paris 75005 France

³ Department of Biochemistry, University of Hong Kong, Pokfulam, Hong Kong

Correspondence: tranp@mail.med.upenn.edu

Content:

Figure Legends

Figure S1, S2, S3, S4

Table S1

Figure Legends

Figure S1.

A. Colony growth in the presence of the microtubule-depolymerizing drug MBC. *csi2Δ* cells are more sensitive to MBC than wildtype cells, indicating defects in the microtubule cytoskeleton.

B. Time-lapse images of a mitotic *csi1Δ* cell expressing mCherry-atb2p (tubulin). The *csi1Δ* cell shows transient microtubule protrusions indicating monopolar spindle phenotype (time=1-9 min), and delayed bipolar spindle formation (time = 10 min). Scale bar, 5μm.

C. Box and dot plot comparison of kinesin-5 cut7p spindle recruitment at mitosis onset in wildtype and *csi2Δ* cells. cut7p organizes spindle bipolarity (Hagan and Yanagida, 1992), and shows similar spindle recruitment time for both wildtype and *csi2Δ* cells, - 3.8±1.2 min (n=23) WT versus -3.6±2.2 min (n=16) *csi2Δ* (p=0.67), suggesting that the *csi2Δ* phenotype is not due to the improper recruitment of cut7p.

D. Box and dot plot comparison of bipolar spindle formation time subsequent to kinesin-5 cut7p recruitment. Wildtype cells establish spindle bipolarity 5.1±1.4 min (n=32) after cut7p recruitment. In contrast, *csi2Δ* cells take 7.4±2.0 min (n=15) ($p < 10^{-3}$).

Figure S2.

A. Time-lapse images showing centromere segregation in wildtype and *csi2Δ* cells expressing mCherry-atb2p and CEN1-GFP (centromere marker on chromosome 1). At anaphase B, when the spindle exhibits a dramatic increase in length, the wildtype centromeres are completely segregated to opposite spindle poles. In contrast, there is a lagging centromere (yellow arrow head) in the *csi2Δ* cell. Bar, 5μm.

B. Box and dot plot comparison of the duration of prophase-metaphase for wildtype and *csi2Δ* cells. Wildtype prophase-metaphase duration is 16.7 ± 3.0min (n=19), similar to 19.1±4.6min (n=20) for *csi2Δ* (p=0.06).

C. Spot assay of cell survival. Single deletion *csi2Δ*, *mad2Δ*, *bub3Δ* and *mph1Δ* grow similarly as wildtype under all temperatures tested. The double-deletion *csi2Δmad2Δ*, *csi2Δbub3Δ* and *csi2Δmph1Δ* exhibit increasing temperature sensitivity and are dead at 37°C, suggesting that the SAC helps ensure proper kinetochore-microtubule attachment in the absence of *csi2p*.

Figure S3.

A. Images of wildtype cells expressing *csi2*-GFP and *sid4*-mRFP (an SPB marker). *csi2*p localizes with *sid4*p at the SPB. Scale bar, 5 μ m.

B. Bar plot comparison of spindle structure in wildtype, *csi1* Δ , *csi2* Δ , and double-deletion *csi1* Δ *csi2* Δ cells expressing mCherry-*atb2*p. Compared to *csi2* Δ , *csi1* Δ cells showed a much higher frequency of transient monopolar spindles. The double-deletion *csi1* Δ *csi2* Δ showed similar frequency of monopolar spindles as *csi1* Δ , suggesting that *csi1*p is dominant over *csi2*p.

Figure S4.

A. Images of monopolar spindles of *cut7.24*^{ts} (control) and *cut7.24*^{ts}*csi2* Δ cells expressing mCherry-*atb2*p. Bottom panels show enlargements of the spindles from the top panels. Yellow dashed lines outline the spindle and microtubule contour, used to measure spindle area and microtubule intensity. Scale bar, 1 μ m.

B. Box and dot plot comparison of control and *csi2* Δ monopolar spindle size. Control cells have spindle size of 158 \pm 22 sq. pixel (n=24). In contrast, *csi2* Δ cells have spindle size of 114 \pm 39 sq. pixel (n=16), or 28% smaller than control (p<10⁻³).

C. Box and dot plot comparison of control and *csi2* Δ spindle microtubule intensity (arbitrary unit). Control cells have microtubule intensity of 2951 \pm 615 a.u. (n=24). In contrast, *csi2* Δ cells have microtubule intensity of 2009 \pm 526 a.u. (n=16), or 32% less than control (p<10⁻³).

Table S1. List of Strains

Strains	Genotype
Figure 1	
PT.1939	mCherry-atb2:HygR leu1-32 ura4-D18 h-
PT.2469	csi2Δ:NatR mCherry-atb2:HygR leu1-32 ura4-D18 h-
PT.2667	mCherry-atb2:HygR alp4-GFP:KanR leu1-32 ura4-D18 h?
PT.2671	csi2Δ:NatR mCherry-atb2:HygR alp4-GFP:KanR leu1-32 ura4-D18 h?
PT.2973	cut7-3GFP:KanR mCherry-atb2:HygR leu1-32 ura4-D18 h-
PT.2975	csi2Δ:NatR cut7-3GFP:KanR mCherry-atb2:HygR leu1-32 ura4-D18 h-
Figure 2	
PT.2482	cdc13-GFP:KanR mCherry-atb2:HygR leu1-32 ura4-D18 h+
PT.2483	csi2Δ:NatR cdc13-GFP:KanR mCherry-atb2:HygR leu1-32 ura4-D18 h+
PT.2489	mini chromosome (ch16; ade6-210; his2) ade6-210 leu1-32 ura4-D18 h+
PT.2490	csi2Δ:NatR mini chromosome (ch16; ade6-210; his2) ade6-210 leu1-32 ura4-D18 h-
PT.2513	mis12-GFP:Leu2 mCherry-atb2:HygR h+
PT.2480	csi2Δ:NatR mis12-GFP:Leu2 mCherry-atb2:HygR h-
Figure 3	
PT.2505	csi2-GFP:NatR mCherry-atb2:HygR leu1-32 ura4-D18 h-
PT.3113	sad1-YFP:KanR csi2-mCherry:NatR ade6-210 leu1-32 ura4-D18 h?
PT.2432	csi2-mCherry:NatR ade6-210 leu1-32 ura4-D18 h-
PT.2673"	csi2-mCherry:NatR sat1.1ts ade6-210 leu1-32 ura4-D18 h?
PT.2649	csi2Δ:NatR sad1-YFP:KanR ade6-210 leu1-32 ura4-D18 h-
PT.2688	csi2-GFP:NatR csi1Δ:KanR mCherry-atb2:HygR ura4-D18 h?
CF.671	csi1-GFP:KanR mCherry-atb2:HygR leu1-32 ura4-D18 h-
PT.2687	csi2Δ:NatR csi1-GFP:KanR mCherry-atb2:HygR leu1-32 ura4-D18 h?
PT.2513	mis12-GFP:Leu2 mCherry-atb2:HygR h+
CF.682	csi1Δ:KanR mis12-GFP:Leu2 mCherry-atb2:HygR ura4-D18 h-
PT.2480	csi2Δ:NatR mis12-GFP:Leu2 mCherry-atb2:HygR h-
Figure 4	
PT.2480	csi2Δ:NatR mis12-GFP:Leu2 mCherry-atb2:HygR h-
PT.3182	cdc13-GFP:KanR mis6-2mRFP-HygR h-
PT.3186	csi2Δ:NatR cdc13-GFP:KanR mis6-2mRFP-HygR h-
Figure 5	
CF.341	cut7.24ts mCherry-atb2:HygR leu1-32 ura4-D18 h+
PT.3134	csi2Δ:NatR cut7.24ts mCherry-atb2:HygR leu1-32 ura4-D18 h-
PT.3138	cut7.24ts mis12-GFP:Leu2 mCherry-atb2:HygR h-
PT.3141	csi2Δ:NatR cut7.24ts mis12-GFP:Leu2 mCherry-atb2:HygR h+
Figure S1	
CF.684	csi1Δ:KanR mCherry-atb2:HygR leu1-32 ura4-D18 h+
PT.2973	cut7-3GFP:KanR mCherry-atb2:HygR leu1-32 ura4-D18 h-
PT.2975	csi2Δ:NatR cut7-3GFP:KanR mCherry-atb2:HygR leu1-32 ura4-D18 h-
PT.286	wildtype ade6-210 leu1-32 ura4-D18 h-
PT.2400	csi2Δ:NatR ade6-210 leu1-32 ura4-D18 h-

Figure S2

PT.2482 cdc13-GFP:KanR mCherry-atb2:HygR leu1-32 ura4-D18 h+
PT.2483 csi2Δ:NatR cdc13-GFP:KanR mCherry-atb2:HygR leu1-32 ura4-D18 h+
CF.441 his7+::LacI-GFP lys1+LacO mCherry-atb2:HygR leu1-32 ura4-D18 h+
PT.2696 csi2Δ:NatR his7+::LacI-GFP lys1+LacO mCherry-atb2:HygR leu1-32 ura4-D18 h+
PT.286 ade6-210 leu1-32 ura4-D18 h-
PT.2400 csi2Δ:NatR ade6-210 leu1-32 ura4-D18 h-
PT.3006 mad2Δ:KanR ade6-210 leu1-32 ura4-D18 h+
PT.3005 bub3Δ:KanR ade6-210 leu1-32 ura4-D18 h+
PT.3004 mph1Δ:KanR ade6-210 leu1-32 ura4-D18 h+
PT.2513 mis12-GFP:Leu2 mCherry-atb2:HygR h+
PT.2481 csi2Δ:NatR mis12-GFP:Leu2 mCherry-atb2:HygR h+
PT.3016 mad2Δ:KanR csi2Δ:NatR mis12-GFP:Leu2 mCherry-atb2:HygR h-
PT.3014 bub3Δ:KanR csi2Δ:NatR mis12-GFP:Leu2 mCherry-atb2:HygR h-
PT.3012 mph1Δ:KanR csi2Δ:NatR mis12-GFP:Leu2 mCherry-atb2:HygR h-

Figure S3

PT.2646 csi2-GFP:NatR sid4-mRFP::ura leu1-32 h?
CF.684 csi1Δ:KanR mCherry-atb2:HygR leu1-32 ura4-D18 h+
PT.1939 mCherry-atb2:HygR leu1-32 ura4-D18 h-
PT.2469 csi2Δ:NatR mCherry-atb2:HygR leu1-32 ura4-D18 h-
PT.2684 csi1Δ:KanR csi2Δ:NatR mCherry-atb2:HygR leu1-32 ura4-D18 h?

Figure S4

CF.341 cut7.24ts mCherry-atb2:HygR leu1-32 ura4-D18 h+
PT.3134 csi2Δ:NatR cut7.24ts mCherry-atb2:HygR leu1-32 ura4-D18 h-
PT.3138 cut7.24ts mis12-GFP:Leu2 mCherry-atb2:HygR h-
PT.3141 csi2Δ:NatR cut7.24ts mis12-GFP:Leu2 mCherry-atb2:HygR h+

Figure S1, Costa et al

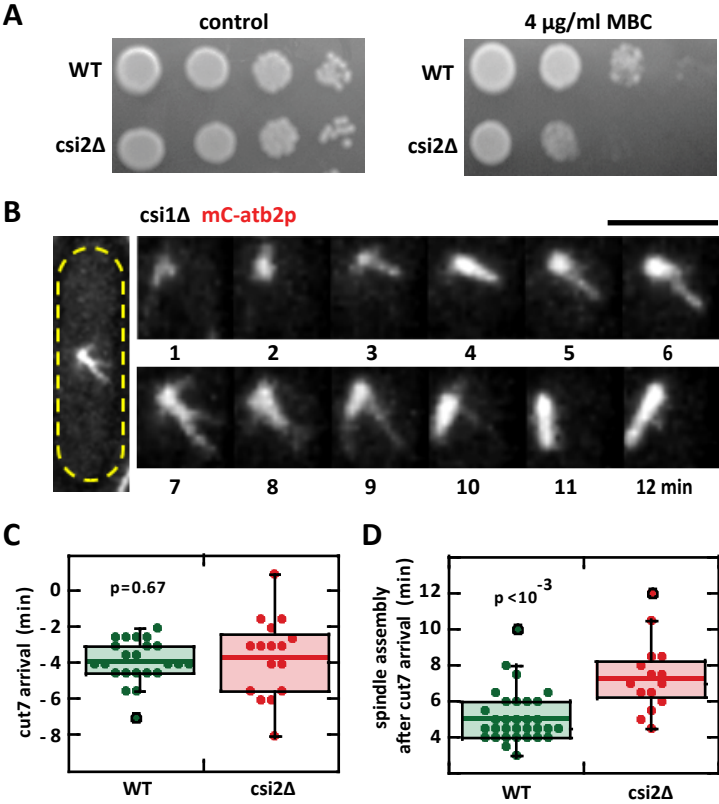


Figure S2, Costa et al

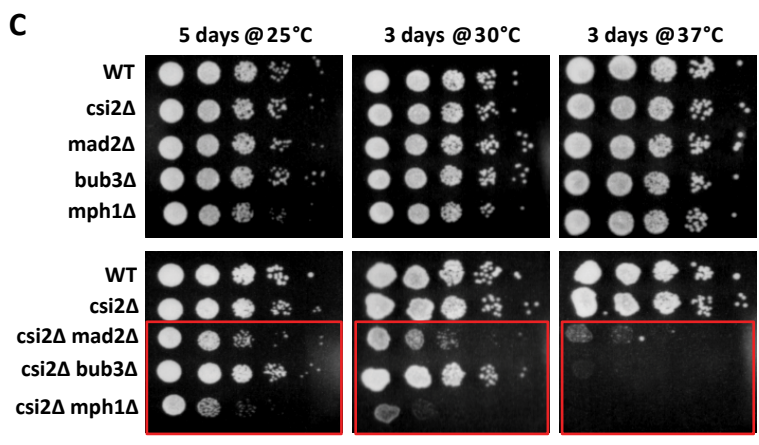
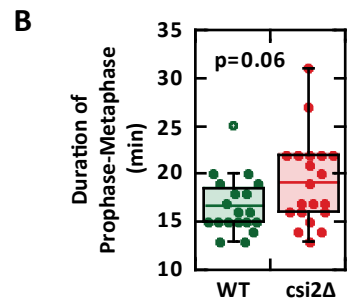
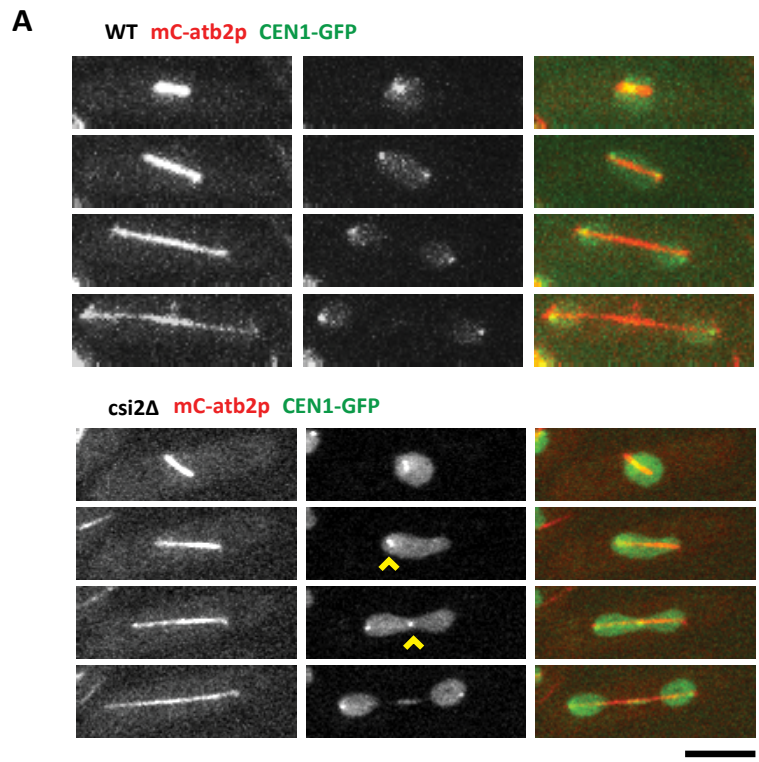


Figure S3, Costa et al

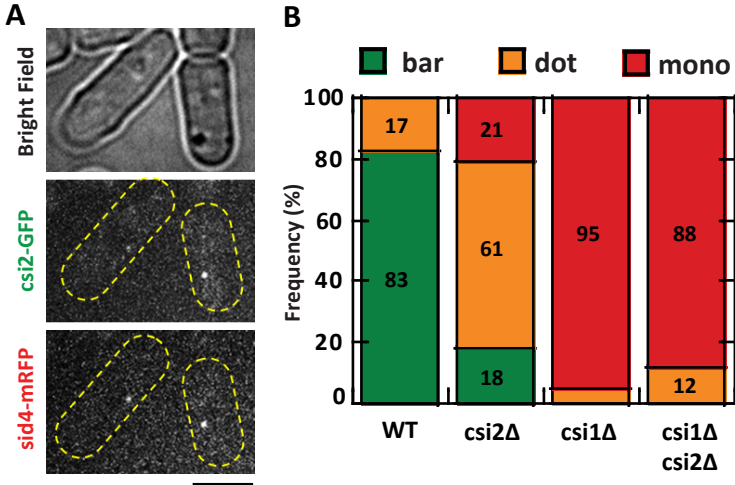


Figure S4, Costa et al

